Astronomical calibration and global correlation of the Santonian (Cretaceous) based on the marine carbon-isotope record

N. Thibault[1], I. Jarvis[2], S. Voigt[3], A. S. Gale[4], K. Attree[2], and H. C. Jenkyns[5]

[1] Department of Geosciences and Natural Resource Management, University of Copenhagen, Øster Voldgade 10, DK-1350, Denmark, nt@ign.ku.dk

[2] Department of Geography and Geology, School of Natural and Built Environments, Kingston University London, Penrhyn Road, Kingston upon Thames, Surrey KT1 2EE, UK

[3] Institute of Geosciences, Goethe-University of Frankfurt, Altenhöferallee 1, 60439 Frankfurt, Germany

[4] School of Earth and Environmental Sciences, University of Portsmouth, Burnaby Building, Burnaby Road Portsmouth PO1 3QL, UK

[5] Department of Earth Sciences, University of Oxford, South Parks Road, Oxford OX1 3AN, UK

Corresponding author: Nicolas Thibault (nt@ign.ku.dk)

This article has been accepted for publication and undergone full peer review but has not been through the copyediting, typesetting, pagination and proofreading process which may lead to differences between this version and the Version of Record. Please cite this article as doi: 10.1002/2016PA002941

Key Points:

- New Upper Coniacian–Lower Campanian high-resolution carbon and oxygen-isotope records for the English Chalk
- Astronomical calibration and global correlation of the Santonian stage
- 405 kyr insolation forcing of carbon-isotope variations via $CaCO_3$ vs. C_{org} burial on land and in oceanic basins

Abstract

High-resolution records of bulk carbonate carbon-isotopes have been generated for the Upper Coniacian to Lower Campanian interval of the sections at Seaford Head (southern England) and Bottaccione (central Italy). An unambiguous stratigraphic correlation is presented for the base and top of the Santonian between the Boreal and Tethyan realms. Orbital forcing of carbon- and oxygen-isotopes at Seaford Head points to the Boreal Santonian spanning five 405 kyr cycles (Sa1 to Sa5). Correlation of the Seaford Head time scale to that of the Niobrara Formation (Western Interior Basin) permits anchoring these records to the La2011 astronomical solution at the Santonian–Campanian (Sa/Ca) boundary, which has been recently dated to 84.19±0.38 Ma. Among the five tuning options examined, option 2 places the Sa/Ca at the 84.2 Ma 405 kyr insolation minimum and appears as the most likely. This solution indicates that minima of the 405 kyr filtered output of the resistivity in the Niobrara Formation correlate to 405 kyr insolation minima in the astronomical solution and to maxima in the filtered $\delta^{13}C$ of Seaford Head. We suggest that variance in $\delta^{13}C$ is driven by climate forcing of the proportions of $CaCO_3$ versus organic carbon burial on land and in oceanic basins. The astronomical calibration generates a 200 kyr mismatch of the Coniacian–Santonian boundary age between the Boreal Realm in Europe and the Western Interior, due either to diachronism of the lowest occurrence of the inoceramid *Cladoceramus*

undulatoplicatus between the two regions, or to remaining uncertainties of radiometric dating and cyclostratigraphic records.

Keywords: Santonian, carbon-isotope stratigraphy, cyclostratigraphy, astronomical calibration

1. Introduction

During the last 10 years, the Late Cretaceous timescale has been improved by integration of floating astronomical time scales (ATS), higher resolution biostratigraphic frameworks, high-resolution carbon-isotope stratigraphy and more accurate and precise radioisotopic dates [*Jarvis et al.*, 2006; *Batenburg et al.*, 2012; *Meyers et al.*, 2012; *Gradstein et al.*, 2012; *Thibault et al.*, 2012a, b; *Voigt et al.*, 2012; *Sprovieri et al.*, 2013; *Sageman et al.*, 2014]. A recent compilation of *Laurin et al.* [2015] proposed a new chronology for an Albian to Campanian carbon-isotope curve, supported by cyclostratigraphy and radioisotopic ages, which revealed the presence of a c. 1.1 myr long-term Milankovitch cycle. The most widely used Late Cretaceous $\delta^{13}C$ reference curve is based on the English Chalk record, and this has proved to be a powerful tool for long-distance correlation [*Jarvis et al.*, 2002, 2006, 2015; *Voigt et al.*, 2010, 2012]. However, the magnitude of post-Turonian carbon-isotope variance is relatively small, and therefore the resolution of the English Chalk $\delta^{13}C$ curve still requires improvement and independent confirmation in other sections. Furthermore, there is a lack of direct orbital calibration of the English Chalk curve to the 405 kyr Milankovitch stable eccentricity target of Laskar (e.g. *Laskar et al.* [2011]).

Correlation problems have been exacerbated by the absence of agreed definitions of the Coniacian–Santonian and Santonian–Campanian Stage boundaries. The Coniacian–Santonian boundary has now been formalized, with a Global Boundary Stratotype Section and Point (GSSP) at Olazaguta, northern Spain [*Lamolda et al.*, 2014]; the defining marker is the lowest occurrence of the inoceramid bivalve *Cladoceramus undulatoplicatus* (Römer), which occurs widely in the northern hemisphere. However, detailed correlation with deep-water Tethyan successions (which generally lack inoceramid bivalves), where the base of the Santonian is traditionally taken at the lowest occurrence of the planktic foraminifera *Dicarinella asymmetrica* (Sigal) [*Premoli Silva and Sliter*, 1994], is not currently possible. There is no formal agreement on either a marker or a type-locality for the Santonian–Campanian boundary GSSP, for which a series of potential markers have been discussed [*Birkelund et al.*, 1984; *Gale et al.*, 1995, 2008], including the base of magnetochron 33R, the highest occurrence (HO) of the crinoid *Marsupites,* the lowest occurrence (LO) of the planktic foraminifera *Globotruncanita elevata* (Brotzen), and the LO of *Dicarinella asymmetrica*.

The $\delta^{13}C$ record plays an important role in the resolution of these debates, as both stage boundaries appear to exhibit positive excursions that constitute robust additional stratigraphic markers [*Jarvis et al.*, 2002, 2006; *Voigt et al.*, 2010]. Here, we present a correlation of new high-resolution carbon-isotope datasets through the Santonian and Lower Campanian of the Boreal (Seaford Head, England) and Tethyan (Gubbio, Italy) realms (Fig. 1, supplementary material), and provide the first attempt to calibrate the new Boreal Santonian $\delta^{13}C$ curve to the recent Astronomical Time Scale (ATS) of the Niobrara Formation in the U.S. Western Interior Basin [*Sageman et al.*, 2014]. This study brings new insights into the presence of condensed levels and potential hiatuses in existing European records, and provides evidence

of the position of the Santonian–Campanian boundary in the standard Tethyan magneto- and biostratigraphic record of Gubbio.

2. Material and methods

2.1. Study sections

2.1.1. Seaford Head, East Sussex, England

Seaford Head is situated on the East Sussex coast between Brighton and Eastbourne, and the cliff section exposes a continuous succession of soft, white nannofossil chalks of Coniacian to Campanian age, typical of this interval in the central Anglo-Paris Basin [*Mortimore*, 1986; *Mortimore and Pomerol*, 1987]. The whole succession is well dated by calcitic macrofossils [*Mortimore*, 1986] and by calcareous nannofossil and foraminifera biostratigraphy (mostly benthic, [*Hampton et al.*, 2007]). *Jenkyns et al.* [1994] published the first bulk oxygen and carbon stable-isotope data for the Middle Santonian to Lower Campanian of the section. *Jarvis et al.* [2006] provided a new summary log for Seaford Head that is adopted here (Fig. 2), and presented at higher resolution in Appendix 1. As previously described by *Mortimore* [1986], *Jenkyns et al.* [1994], *Jarvis et al.* [2006] and *Hampton et al.* [2007], the lithostratigraphy of the section is well established and includes a large number of characteristic regional named marker beds, mostly corresponding to marly chalk beds, distinctive flint layers and beds of fossils (Fig. 2, Appendix 1). The section was previously considered as a potential candidate GSSP for the Coniacian–Santonian and Santonian–Campanian boundaries, and thus constitutes an excellent stratigraphic standard for the Santonian of NW Europe [*Hancock and Gale*, 1996; *Lamolda and Hancock*, 1996].

A new bulk carbonate carbon and oxygen stable-isotope record from 364 samples taken at 25 cm intervals is presented here for the uppermost Coniacian to lowermost Campanian succession (91 m thick; 50.7610°N 0.1149°E – 50.7636°N 0.1108°E).

2.1.2. Bottacione Gorge, Gubbio, Umbria, Italy

The two classic sections of the Bottaccione Gorge and Contessa Highway near the medieval city of Gubbio (central Italy) constitute the standard reference for the Upper Cretaceous to Paleocene of the Tethys, thanks to their sequence of polarity magnetozones correlated to calcareous nannofossil and planktic foraminifer zonations. These sections have also been considered as potential stratotypes or reference sections for the definition of the Santonian–Campanian and Campanian–Maastrichtian boundaries [*Monechi and Thierstein*, 1985; *Gardin et al.*, 2001, 2012; *Petrizzo et al.*, 2011].

Sprovieri et al. [2013] and *Coccioni and Premoli-Silva* [2015] recently presented syntheses for the Upper Albian–Maastrichtian of the Gubbio succession, compiling planktonic foraminifera and calcareous nannofossil biostratigraphy, magnetostratigraphy and high-resolution carbon-isotope stratigraphy. However, the published carbon-isotope records of the Santonian at Gubbio [*Jenkyns et al.*, 1994; *Sprovieri et al.*, 2013] still lack a sufficiently high resolution to permit unambiguous correlation of the uppermost Coniacian to lowermost Campanian carbon-isotope excursions to those recognized in NW Europe.

In the present study, new bulk carbonate carbon-isotope records of the Upper Coniacian to Lower Campanian of the Bottaccione section have been generated, two along the road (43.3621°N 12.5825°E 571 m altitude) and one along the river. Our ‘Road’ section records comprise two new data sets: a low-resolution set of 108 samples spanning the Middle

Coniacian – Upper Campanian (104 m thick section) supplied by Prof. Isabella Premoli Silva, collected at approximately 1 m intervals; and a high-resolution set of 78 samples taken every 25 cm across the Santonian–Campanian boundary interval (19.25 m, thick). The new 'River' section is located opposite the road section in the Bottaccione Gorge valley. The upper Coniacian to lowermost Campanian part of the succession is exposed along the valley wall (43.3626°N 12.5820°E – 43.3630°N 12.5824°E) and continues with a small gap of exposure in the creek for the higher Campanian part (43.3630°N 12.5826°E – 43.3635°N 12.5830°E). The River section data comprise 326 samples taken at 25-cm resolution through the Middle Coniacian–Upper Campanian (total thickness: 88.5 m), except for the interval between 226 and 233 m, which was inaccessible.

2.2. Stratigraphic revisions

The macrofossil biostratigraphy of the Seaford Head section is revised here using our own records from the section, and is correlated at a bed scale to the lithostratigraphy (Fig. 2, Appendices 1 and 2). Calcareous nannofossil and foraminifer data have been derived from *Hampton et al.* [2007]. For Seaford Head and the other English sections discussed below, we use the modified North Sea UC nannofossil scheme of *Fritsen* [1999]. In this study, the adopted nomenclature for biostratigraphic events is the use of lowest occurrences (LO) and highest occurrences (HO) instead of the commonly used first and last occurrences, respectively. This is because this adopted nomenclature does not imply any notion of time and applies strictly to stratigraphic layers of particular sections or areas. Despite not being officially ratified by the International Commission on Stratigraphy, we adopted an upper case notation for Lower, Middle and Upper stage subdivisions of Late Cretaceous stages, following the style of the Geologic Time Scale 2012 (*Gradstein et al.*, 2012) but also because such a notation gives room for further informal subdivisions (e.g. lower Lower, upper Lower,

etc.). For practical reasons, we did not follow the recommendations of *Holden et al.* (2011) and adopted a clear distinction between time (ka, Ma) and time span units (kyr, myr).

Hampton et al. [2007] placed the base of UC14iii at Seaford Head at the HO of *Cylindralithus crassus* (Fig. 3), according to the scheme of *Fritsen* [1999]. The LO of *Monomarginatus quaternarius* situated 2 meters above the HO of *C. crassus* can be used as a marker for the base of UC15 sensu *Burnett et al.* [1998]. According to *Burnett et al.* [1998], the base of UC15 is defined by the LO of *Misceomarginatus pleniporus*, a rare species which is almost undistinguishable from *M. quaternarius* in moderately preserved material, and considered to be a possible synonym of the latter species. *Burnett et al.* [1998] regarded the LO of *M. quaternarius* as a secondary marker for the base of UC15, and it is recommended here as the best marker for the base of this zone in the Boreal realm, as this species is present in a large part of the Chalk sea: in England, in the Danish Basin and in North Germany [*Schönfeld et al.*, 1996; *Hampton et al.*, 2007; *Thibault et al.*, 2012b; Fig. 3]. Accordingly, the LO of *M. quaternarius* at Trunch indicates the base of UC15 (Fig. 3). The definition of the base UC15 by the HO of *Saepiovirgata biferula* (a rare holococcolith species) used in the *Fritsen* [1999] scheme should rather be applied strictly to North Sea sites where *M. quaternarius* appears to be absent.

The calcareous nannofossil zonation at Gubbio has been revised using the standard UC^{TP} zonation of *Burnett et al.* [1998] for Tethyan and intermediate provinces, based on original data on biohorizons given in *Monechi and Thierstein* [1985], *Gardin et al.* [2001] and in the recent compilation of *Coccioni and Premoli-Silva* [2015]. For the Lägerdorf reference section in NW Germany [*Schulz et al.*, 1984], discussed below, we applied the standard UC^{BP} zonation of *Burnett et al.* [1998] for the Boreal Realm based on original data on biohorizons given in *Schönfeld et al.* [1996].

2.3. Methods

2.3.1. Bulk oxygen and carbon stable isotopes

At Seaford Head, samples of ~1 kg were collected during 2006 at 25 cm intervals through a 91 m thick section. Subsamples of around 50 g were crushed to < 3 mm chips in clean thick-walled plastic bags, using a metal plate and hammer. The chips were hand ground to a fine powder in an agate pestle and mortar. Carbon and oxygen stable-isotope analyses of the bulk carbonate fraction ($\delta^{13}C$, $\delta^{18}O$) in 250 μg of powdered samples were performed in the stable-isotope laboratory of the Department of Earth Sciences, Oxford University, using a VG Isogas Prism II mass spectrometer with an on-line VG Isocarb common acid bath preparation system. Samples were first cleaned using hydrogen peroxide and acetone and dried at 60°C for at least 30 minutes. In the instrument they were reacted with purified phosphoric acid at 90°C. Calibration to the Vienna Peedee belemnite (VPDB) standard via NBS-19 was made daily using the Oxford in-house (NOCZ) Carrara marble standard. Data are reported in delta (δ) notation as per mil (‰) relative to VPDB. Reproducibility of replicate standards was better than 0.1‰ for $\delta^{13}C$ and $\delta^{18}O$.

At Bottaccione, samples were collected along two sections, the Road and the River, during two different field campaigns. Uppermost Santonian to Lower Campanian strata of the road section were sampled at 25 cm spacing in 2008. The River section, which exposes the uppermost Coniacian to lowermost Upper Campanian, was sampled at 25 cm spacing in 2008 and 2010. A complementary low-resolution set of Coniacian – Lower Campanian samples from Bottaccione Road, spaced at 1 m intervals, was kindly provided by Prof. Isabella Premoli Silva. Each sample for stable-isotope analysis was drilled from rock pieces with a hand-held drill bit (1 mm diameter) to avoid secondary calcite in microfractures and stylolites. Samples collected in 2008 along the Bottaccione Road and River sections were

analysed in the stable-isotope laboratory at Oxford University using the methods described above. Samples collected in 2010 and those provided by Prof. Premoli Silva were analysed in the stable-isotope laboratory at Frankfurt University. In Frankfurt, stable-isotope analyses of bulk carbonates were performed at a reaction temperature of 72°C using a Finnigan MAT 253 with Gasbench. All isotope values are reported in ‰ VPDB. The reproducibility of repeated standard measurements was better than 0.07 ‰ and 0.02 ‰ for oxygen and carbon isotopes, respectively.

2.3.2. Cyclostratigraphy

The cyclostratigraphic analysis was performed on carbon- and oxygen-isotope variations in the depth and in the time domains after orbital tuning of the time-series. Prior to the spectral analysis, long-term trends of the $\delta^{13}C$ signal were removed from the original signal using a piecewise linear interpolation of the time-series. This interpolation allows for a linear detrending on several portions of the time-series based on a least-square interpolation with break points defined at 8.75, 32.75, 50.75, 57.00 and 75.50 m, which correspond to maxima and minima of observed long-term trends (Fig. 4). Similar spectra were obtained when detrending long-term trends using different robust loess smoothing weighted averages over 40 to 60% of the total time-series, but the power of the identified frequencies were systematically higher and better expressed when detrending with the piecewise linear interpolation.

Orbitally tuned time-series were reinterpolated at 5 kyr steps. Spectral analyses were performed using the Multi-Taper Method (MTM) with a red noise simulation from *Schulz and Mudelsee* [2002] developed for Matlab™ by *Husson et al.* [2014]. The red noise simulation allows the estimation of confidence levels based on a Chi-square statistical test performed on the theoretical spectrum of the red noise. Chi2 confidence levels are based on

an AR1 autocorrelation model built on 1000 Monte Carlo simulations. An Average Spectral Misfit (ASM) method was tested on the $\delta^{13}C$ for the 40.00 to 90.75 m interval where sedimentation rates were considered to be more stable (see Results, below).

ASM is a robust inverse method from the Astrochron package [*Meyers*, 2014] allowing testing of the alignment and fit between observed spectral peaks of a sedimentary time-series and several target orbital frequencies from the Laskar astronomical solution [*Laskar et al.*, 2004], using a range of plausible sedimentation rates [*Meyers and Sageman*, 2007]. The ASM methodology allows identification of an optimal sedimentation rate, which minimizes the misfit between the observed frequencies of the sedimentary record and the orbital frequency targets. However, this method can only be tested on time-series with relatively constant sedimentation rates [*Meyers and Sageman*, 2007]. Significance levels for rejection of the null hypothesis of the ASM (no orbital signal) are estimated with Monte Carlo spectra simulations [*Meyers et al.*, 2012].

In addition, Evolutive Harmonic Analysis (EHA) was applied with a step of 5 kyr and a window of 500 kyr to the time-series tuned to the 405 kyr component using the script of *Meyers et al.* [2001] provided in the Astrochron package [*Meyers*, 2014]. In order to extract the potential cyclicities identified by the cyclostratigraphic analysis, we used Taner filters [*Taner*, 2000] for high-precision extraction of specific astronomical frequency targets.

3. Results

3.1. Isotopic trends

3.1.1. Seaford Head

Major carbon isotopic events and medium-term trends through the Middle Coniacian to Lower Campanian at Seaford Head were described by *Jarvis et al.* [2006] based on the low-resolution bulk carbonate $\delta^{13}C$ curve of *Jenkyns et al.* [1994] for the Middle Santonian–Lower Campanian interval, plus lithostratigraphic correlation to other English sections. In the present study, the Seaford isotope curve has been extended down into the Middle Coniacian and its resolution significantly improved, but all isotopic excursions previously defined and correlated to the lithostratigraphy and macrofossil biostratigraphy remain essentially unchanged (Fig. 2, *Jarvis et al.* [2006]).

Precise calcareous nannofossil and regional benthic foraminiferal biozonations were established at Seaford Head by *Hampton et al.* [2007], and these are shown with the revised macrofossil biostratigraphy, our new carbon-isotope curve and the carbon-isotope event (CIE) stratigraphy in Figure 2. Carbon-isotope values typically range between 2.0 and 2.6 ‰, with no clear long-term trend upwards. Small short-term (meter-scale) low-amplitude (0.2 ‰) peaks and troughs are superimposed on medium-term (decameter) higher amplitude (0.6 ‰) cycles.

Prominent positive $\delta^{13}C$ excursions associated with medium-term carbon-isotope maxima are the Kingsdown and Horseshoe Bay CIEs in the upper Middle Coniacian and upper Middle Santonian, and the double peak of the Santonian–Campanian Boundary Event (SCBE, Fig. 2). Negative excursions associated with medium-term $\delta^{13}C$ minima are the Haven Brow and Buckle CIEs in the lower Middle Santonian and basal Upper Santonian, respectively. Key macrofossil biostratigraphic datum levels include: the LO *C. undulatoplicatus* marking the

base of the Santonian, which occurs at the top of the Michel Dean positive CIE; the LO *Uintacrinus socialis* marking the base of the Upper Santonian, which is located a short distance below the $\delta^{13}C$ minimum defining the Buckle CIE; and the HO *Marsupites* defining the base Campanian, which occurs at the top of the lower peak (a) of the SCBE doublet (Fig. 2).

3.1.2. Gubbio

A thorough description of the Upper Albian–Lower Campanian carbon isotope curve of the Bottaccione reference section was provided by *Sprovieri et al.* [2013]. However, the new high-resolution records established here for the Tethyan Upper Coniacian to Lower Campanian of the Bottaccione River and Road sections call for a revision of *Sprovieri et al.*'s [2013] interpretation of the isotopic events through this interval. In those authors' interpretation, the small 0.2 ‰ positive excursion correlated to the C33R/C33N boundary was interpreted as the Santonian–Campanian Boundary Event, whereas the long-term 0.4 ‰ positive excursion correlated with the C34N/C33R boundary was interpreted as the Horseshoe Bay CIE (Fig. 5). A similar erroneous correlation was proposed in Figure 14 of *Jarvis et al.* [2006] whereas *Wendler* [2013] proposed a correlation similar to our new interpretation. Those erroneous interpretations were due to insufficient resolution and high-amplitude scatter (typically 0.3 – 0.5 ‰) in the *Sprovieri et al.* [2013] dataset, that prevented recognition of the true Horseshoe Bay Event within the top of C34N, immediately above the LO *G. elevata* (Fig. 5).

Carbon-isotope values in the Bottaccione succession typically range between 2.2 and 2.8 ‰, with highest values at the base of the sections, in the Coniacian (Fig. 5). An offset of 0.1 ‰ in absolute values between the similarly shaped low- and high-resolution Bottaccione Road curves is attributed to a systematic inter-laboratory bias. Correlation of our Gubbio curves to

the Boreal Campanian reference section at Lägerdorf [*Schulz et al.*, 1984; *Schönfeld* et al., 1996; *Voigt et al.*, 2010] is shown in Figure 5. Major Middle Coniacian–Lower Campanian CIEs from the Kingsdown to the SCBE can be confidently correlated between the two sections. For the higher Campanian, the key tie point is the positive $\delta^{13}C$ excursion at the top of our low-resolution data set, which is equated to the Mid-Campanian CIE of *Jarvis et al.* [2002], based on its position immediately below the LO *Radotruncana calcarata* (Cushman). This interval is correlated with the well-defined $\delta^{13}C$ peak in the lower *basiplana/spiniger* Zone at Lägerdorf. Above this level, the carbon-isotope profile begins a long-term fall (Fig. 5), interpreted to represent the start of the falling trend that ultimately leads to a well-developed negative excursion, the Late Campanian CIE, in the mid-Upper Campanian [*Jarvis et al.*, 2002, 2006, 2008; *Voigt et al.*, 2010].

The $\delta^{13}C$ peak at the base of the Upper Campanian at Lägerdorf correlates with a more marked positive excursion at the same biostratigraphic level in the Trunch borehole succession of Norfolk, Eastern England [*Jenkyns et al.*, 1994; *Jarvis et al.*, 2002, 2006]. This peak was previous equated with the Mid-Campanian Event by *Jarvis* et al [2002]; the new data presented here from Bottaccione indicate that it is better correlated with a peak in the mid-*C. plummerae* Zone. The $\delta^{13}C$ peak is differentiated here as the Trunch CIE, which is at the level of the Trunch Hardgrounds in the Norfolk section [*Jarvis et al.*, 2006].

A well-developed peak of ~ 0.2 ‰, coincident with a medium-term $\delta^{13}C$ maximum, occurs in the mid-Lower Campanian *papillosa* Zone at Lägerdorf and in the uppermost *G. elevata* Zone (Chron 33R/33N boundary) at Bottaccione, and two small negative excursions of ~ 0.15 ‰ below this interval can be traced from the *pillula* and *senonensis* Zones at Lägerdorf, to the lower and mid-*G. elevata* Zone at Bottaccione, respectively. However, these excursions have very low amplitudes and their stratigraphic significance will need to be tested in high resolution datasets from other sections. For correlation purposes, the Campanian CIEs

identified here are informally referred to their corresponding macrofossil zonal names in the Lägerdorf section, e.g. *pillula* Zone event (Fig. 5; in this case immediately above the LO *Globotruncanita atlantica* (Caron) at Bottaccione).

3.2. Cyclostratigraphy of the Seaford Head section

3.2.1. Cyclostratigraphy in the depth domain

Results of the Multi-Taper Method spectral analysis on the detrended $\delta^{13}C$ variations of the Seaford Head record highlight one highly significant periodicity at 16 m, a poorly significant peak at 4.2 m, and three other periodicities at 0.75, 0.68 and 0.56 m (Fig. 4). The MTM spectral analysis of the $\delta^{18}O$ signal highlights mainly high-frequency variations with highly significant peaks at periodicities of 4.2 m and 1.18 m, and less significant peaks at 0.75, 0.69 and 0.57 m (Fig. 4). Frequency ratios suggest assignment of the 16 m peak to the 405 kyr eccentricity, of the 4.2 m peak to the 100 kyr eccentricity, of the 1.18 m peak to obliquity, and of the three remaining high-frequency peaks to the precession. Filtering of the 16 m peak highlights the expression of ca. 7.8 long-eccentricity cycles of 405 kyr in the $\delta^{13}C$ signal and ca. 81 obliquity cycles in the $\delta^{18}O$ record (Fig. 4), and points to relatively concordant durations of 3155 and 3078 kyr when tuning the time-series to the 405 kyr eccentricity and 38 kyr obliquity, respectively (Fig. 4).

Results of the filtering and of the two distinct tunings to the 405 kyr eccentricity and 38 kyr obliquity suggest a significant decrease of the compacted sediment accumulation rate from ca. 4 to 2.5 cm/kyr in the interval comprised between 17 and 40 m (Upper Coniacian–mid-Middle Santonian; Fig. 4). Sediment accumulation rate appears to vary slightly around 3 cm/kyr for the remainder of the time-series. Average Spectral Misfit was thus tested on the latter interval comprised between 40.00 and 90.75 m, for which four main significant

frequencies can be recognized in the MTM power spectrum (Fig. 6, Table 1). Results of the ASM support an optimum sediment accumulation rate of 3.05 cm/kyr and suggest assignment of the four main identified frequencies to E405, e2, p1 and p2 (Fig. 6, Table 1). A second ASM evaluating all frequency peaks of the MTM power spectrum of the 40.00 – 90.75 m interval, comprising those below significance levels, provides very similar results with an optimum sediment accumulation rate of 2.97 cm/kyr (Appendix 2).

3.2.2. Cyclostratigraphy in the time domain

Cyclostratigraphic analysis in the time-domain is fundamental because, if the tuning is accurate, then Milankovitch frequencies should be better defined, potentially with higher power in the MTM of the new time-series (Fig. 7). Due to the chaotic behaviour of the solar system, the 405 kyr component of the eccentricity is the only orbital parameter stable throughout the Mesozoic–Cenozoic [*Laskar et al.*, 2004]. Alternatively, the second most suitable Milankovitch component for orbital tuning should be obliquity, because it is a relatively stable component with a narrow and well-defined peak in the Laskar astronomical solution (La2004, *Laskar et al.* [2004], Fig. 7D). Both components are expressed with relatively narrow peaks and very high significance either for the 405 kyr in the $\delta^{13}C$ record or for the obliquity in the $\delta^{18}O$ record (Fig. 4).

We tested two distinct age-models based on the 405 kyr filter output of the ^{13}C data and 38 kyr filter output of the ^{18}O data. The two distinct tuned time-series are not significantly different and have very similar durations. The MTM spectral analysis of the two distinct tuned time-series of the ^{13}C data reveal all expected Milankovitch frequencies but differ significantly with respect to the expression of these frequencies. The 405 kyr tuning logically resolves the 405 kyr component much better and was thus chosen here to highlight

the expression of the 405 kyr cycles in the carbon-isotope record of Seaford Head (Fig. 7). This component is very stable and remains along a straight line in the Evolutive Harmonic Analysis (E in Fig. 7C), although a slight perturbation is observed at around 1000 kyr in the top of E405 Sa1. However, the 405 kyr tuning poorly resolves the remaining Milankovitch frequencies, whose significance is reduced because of the very high power of the 405 kyr component. A 122 kyr component is present in the MTM but below the 90% significance level, the obliquity appears shifted to 34 kyr, and precession components are not highly significant (Fig. 7B).

When the 405 kyr is filtered out, other components are well expressed (Fig. 7G). The 38 kyr tuning of the $\delta^{13}C$ signal resolves much better the high frequencies with an extremely well-defined 38 kyr peak, significant precession components and two poorly significant short-eccentricity peaks at 127 and 91 kyr (Fig. 7E), as expected when compared to the La2004 solution (Fig. 7D). The expression of the 38 kyr peak in the tuned $\delta^{13}C$ record is particularly relevant here as the series was actually tuned on the 38 kyr filter of the $\delta^{18}O$ record, and as this component was not particularly significant in the original MTM power spectrum of the $\delta^{13}C$ in the depth domain (Fig. 4). This analysis reveals that the tuning improved significantly the expression of Milankovitch frequencies.

4. Discussion

4.1. Correlations in the Boreal Realm

Correlation of our high-resolution $\delta^{13}C$ curve for Seaford Head to published lower resolution Boreal $\delta^{13}C$ records for the Coniacian to Campanian of the German and English Chalk is fully consistent with the available macrofossil biostratigraphy for the sections (Fig. 3). The LO *C. undulatoplicatus*, marking the base of the Santonian, is associated with the short-term positive $\delta^{13}C$ excursion of the Michel Dean CIE and falls on a medium-term

falling trend that begins at the level of the HO *V. involutus*. The Buckle CIE occurs immediately above the LO *U. socialis*, and the Foreness CIE above the LO *Marsupites.* The Santonian–Campanian Boundary Event (SCBE) consistently exhibits a well-defined pair of $\delta^{13}C$ excursions at the peak of a broad medium-term carbon-isotope maximum, with the lower peak (SCBE a) being coincident with the HO of *Marsupites testudinarius*, the preferred marker of the stage boundary according to *Gradstein et al.* [2012] (Fig. 3). Correlation of the remainder of the Lower Campanian section is hampered by the lack of a high-resolution record at Seaford Head and elsewhere, very low amplitude $\delta^{13}C$ variation in most sections, and a paucity of correlatable macrofossil datum horizons.

Available calcareous nannofossil data are less consistent with respect to the $\delta^{13}C$ chemostratigraphy. For example, the LO of the calcareous nannofossil *Broinsonia parca parca* is either at the top of, or some distance above the SCBE. This slight mismatch may be due to preservation or taxonomic issues, as "small" and "big" *B. parca parca* have not been clearly depicted elsewhere yet. A potential mismatch is also apparent with respect to the LO of *Calculites obscurus*, which is recorded in the Upper Santonian at Lägerdorf and Trunch but occurs stratigraphically much lower, in the Upper Coniacian, below the Kingsdown Event at Seaford Head. This mismatch was previously discussed by *Burnett et al.* [1998] and *Wagreich* [2012]. Interestingly, *Hampton et al.* [2007] noticed a marked increase in *C. obscurus* within peak 'a' of the SCBE at Seaford Head (Fig. 3). It is likely that the LO of *C. obscurus* at Trunch and Lägerdorf actually corresponds to a lowest common occurrence (LCO) of the species in the Upper Santonian throughout the Boreal realm, and that this species was too rare to be observed below this level in the two latter sections.

4.2. Correlation of Boreal and Tethyan records

Correlation of the new high-resolution $\delta^{13}C$ record of Seaford Head with the new $\delta^{13}C$ records from Gubbio allows for an excellent tie of the Coniacian–Santonian and Santonian–Campanian boundaries between the Boreal and Tethyan realms (Fig. 8). The correlation allows the better identification of the Horseshoe Bay CIE at Gubbio, enabling all the isotopic excursions previously identified in the English Chalk to be placed on the Gubbio record. This correlation also shows that the double peak of the SCBE is a consistent feature that can be observed at Seaford Head, Gubbio and at Lägerdorf (Figs 3, 5–7).

The revised correlation of the Santonian–Campanian boundary between Gubbio and Seaford Head calls for a revision of the magnetostratigraphic interpretation of *Montgomery et al.* [1998] for the English Chalk (Fig. 8). Magnetostratigraphy is a difficult exercise in chalks, which generally lack a sufficiently high concentration of magnetic minerals to provide reliable inclination data [*Hambach in Schönfeld et al.*, 1996]. Combined magnetostratigraphic records from Seaford Head and Culver Cliff (Isle of Wight) led *Montgomery et al.* [1998] to propose a C34N/C33R Chron boundary within the *Uintacrinus socialis* Zone, at the top of the Buckle Marls (immediately above the Buckle CIE), where both records suggest a shift from normal to reverse polarity (Fig. 8). However, our new correlation of the SCBE between Gubbio and Seaford Head demonstrates that this interpretation is erroneous. At Gubbio, which is the Tethyan reference for Late Cretaceous to Paleocene magnetostratigraphy [*Gradstein et al.*, 2012; *Coccioni and Premoli Silva*, 2015], the SCBE lies at the top of Chron C34N, indicating that the base of Chron 33R must lie within the lower *O. pillula* Zone at Seaford Head (Fig. 8). It is concluded that the published English Chalk magnetostratigraphy is unreliable, due to the very weak magnetic signal present, a conclusion that was already reached by *Hampton et al.* [2007] based on *Barchi* [1995].

The Coniacian–Santonian boundary, as defined by the LO of *Cladoceramus undulatoplicatus* at Seaford Head, correlates with the Michel Dean Flint and with the Michel Dean positive carbon-isotope excursion, which can be correlated to Gubbio at ca. 195 m, within the lower part of the *D. asymmetrica* planktonic foraminifer zone and the lower part of nannofossil Zones UC11c^{TP} to UC12 (Fig. 8). This correlation and identification of the Michel Dean CIE at Gubbio is supported by the correlation of the Horseshoe Bay Event in the Santonian, and the Kingsdown CIE in the Upper Coniacian of the two sections (Fig. 8). At the GSSP of Olazagutia, the Coniacian–Santonian boundary has been placed ca. 5 m below the Michel Dean CIE [*Lamolda et al.*, 2014], although the definition and position of the CIE may require modification in the light of our new high-resolution isotope data.

Finally, the correlation of the Gubbio and Seaford Head isotopic records indicates an interval of condensation at Gubbio in the Lower Santonian between 195 and 200 m (Fig. 8). It should be noted that the whole Lower Santonian interval between the Michel Dean and Horseshoe Bay events also appears more condensed at Lägerdorf and Trunch/Dover than at Seaford Head (Fig. 3). The much lower sediment accumulation rate noted at Seaford Head between 17 and 40 m also corresponds to this interval, suggesting a global episode of sediment starvation in the Early Santonian.

4.3. Correlation to the ATS of the Western Interior and astronomical calibration to La2011

The Coniacian–Santonian and Santonian–Campanian boundaries were recently assigned precise radiometric dates by *Sageman et al.* [2014], using interpolation of new $^{40}Ar/^{39}Ar$ and $^{206}Pb/^{238}U$ ages of ash layers in the Niobrara Formation of the Western Interior. An integrated radiometric and orbital time scale was proposed by those authors for the

Coniacian to Lower Campanian interval in the Western Interior [*Locklair and Sageman*, 2008; *Sageman et al.*, 2014]. The 405 kyr filter output of the Niobrara Formation was extracted from a micro-resistivity signal mostly reflecting inverse variations of the siliciclastic fraction [*Locklair and Sageman*, 2008]. However, their 405 kyr filter output was not calibrated to the most recent astronomical solutions [*Laskar et al.*, 2011a, 2011b]. This exercise is performed here by a tie to the La2011 solution which has proved to be the most robust solution so far for the Cenozoic and pre-Cenozoic astronomical calibrations [*Batenburg et al.*, 2012; *Dinarès-Turrell et al.*, 2013, 2014]. La2010d was not considered here because the 405 kyr filter output of this solution, which is the only reliable target for astronomical calibration of pre-Eocene records, is actually very close to that of La2011 and because La2011 shows a better fit to early Cenozoic geological data [*Dinarès-Turrell et al.*, 2014]. Correlation of the Santonian–Campanian boundary between the Tethyan and Boreal realms and the Western Interior is further supported by the finding of the double-peak SCBE positive excursion in organic carbon isotopes across the transition from the *Demoscaphites bassleri* to *Scaphites leei* III ammonite zones in the Aristocrat Angus core (Niobrara Formation, Colorado) [*Joo and Sageman*, 2014].

The Santonian–Campanian boundary, dated at 84.19±0.38 Ma, is characterized by a minimum in the 405 kyr filter output of the resistivity in the Western Interior (Fig. 9). In the English Chalk, the Santonian–Campanian boundary is characterized by a well-defined maximum of the $\delta^{13}C$ 405 kyr filter output (Fig. 9). It is striking that the 405 kyr component of the La2011 astronomical solution also shows a well-defined insolation minimum at exactly 84.2 Ma and this tie appears to be the most likely tuning option to the minimum in resistivity in the Western Interior and maximum in $\delta^{13}C$ in UK (Fig. 9, Option 2). However, the remaining uncertainties in the radiometric dates of the Coniacian–Santonian and Santonian–Campanian boundaries in the Wester Interior call for 5 distinct tuning options to the La2011

solution (Figs. 9–10). Tuning Options 1 to 3 consider a tie of 405 kyr insolation minima to maxima of the $\delta^{13}C$ 405 kyr filter output in UK and minima in the 405 kyr filter output of the resistivity signal in the Wester Interior (Fig. 9). Out of these three possibilities, Options 1 and 3 are less likely as either the projected Coniacian–Santonian boundary or Santonian–Campanian boundary astronomical ages appear to fall slightly out of the uncertainty range in radiometric dates of the Western Interior (Fig. 9, Table 2). Astronomical Option 2 shows by far the best match with radiometric dates (Fig. 9, Table 2).

Tuning Options 4 and 5 consider a tie of 405 kyr insolation maxima to maxima of the $\delta^{13}C$ 405 kyr filter output and minima in the 405 kyr filter output of the resistivity signal in the Wester Interior (Fig. 10). These two options fall well within the range of uncertainties in radiometric dates and can therefore not be discarded (Fig. 10, Table 2). In any case, the correlation presented for these 5 options highlights a mismatch in the position of the Coniacian–Santonian boundary as defined by the LO of *C. undulatoplicatus* between the UK and the Western Interior (Figs. 9–10, Table 2). Depending on the choice of the tuning option, this mismatch accounts for a total of ca. 170 to 210 kyr (Table 2). It remains unclear whether the mismatch is due to a slight diachroneity of the lowest occurrence of *C. undulatoplicatus* between the Boreal realm and the Western Interior or to remaining uncertainties in the radiometric dates and cyclostratigraphic analysis.

4.4. Insolation forcing of carbon-isotope variations

The strong expression of the obliquity expressed in oxygen-isotopes is not particularly surprising for a section that was situated at boreal mid-latitudes in the Santonian and several examples even show a well-expressed obliquity at low latitudes [*Bosmans et al.*, 2015]. The lesser expression of the obliquity observed in carbon-isotopes of Seaford Head may then be

explained by the ca. 200 kyr-long residence time of dissolved inorganic carbon in the ocean [*Zeebe and Wolf-Gladrow*, 2008]. The proposed tuning options of the 405 kyr eccentricity filter output of the Seaford Head $\delta^{13}C$ to the 405 kyr filter output of the resistivity signal in the Niobrara Formation and to the La2011 astronomical solution need to be examined through our current understanding of external forcings (insolation) and internal paleoceanographic responses in individual oceanic basins. *Locklair and Sageman* [2008] demonstrated that the resistivity signal of the Niobrara Formation is mainly a reflection of the carbonate content; the main controlling mechanism of these variations was through the siliciclastic flux to the Western Interior Basin, which was at that time a restricted epicontinental seaway. Such an interpretation could imply that minima of the resistivity (low carbonate intervals) correlate to maxima of insolation due to more intense continental weathering (driving increased siliciclastic and nutrient input) during insolation highs. Such an interpretation would be in favour of tuning Options 4 and 5 and implies a correlation of maxima of insolation to maxima in $\delta^{13}C$, as suggested by the correlation of Figure 10. A possible mechanism would be for the increased nutrient supply to the oceans, driven by increased terrestrial weathering, to promote increased marine productivity and increased marine organic-carbon burial. Sediments deposited in the Western Interior Basin during the Santonian are relatively rich in organic matter [*Tessin et al.*, 2015]. Preferential removal of ^{12}C from the oceans by increased organic matter burial would lead to higher $\delta^{13}C$ values in surface carbon reservoirs [*Scholle and Arthur*, 1980].

By contrast, Options 1 to 3, among which Option 2 shows by far the best match to radiometric dates out of the 5 considered possibilities, imply a correlation of maxima in insolation to maxima in resistivity (high carbonate intervals) in the Niobrara Formation and to minima in $\delta^{13}C$ (Fig. 9). A correlation between minima in bulk carbonate $\delta^{13}C$ and insolation maxima of the 405 kyr eccentricity has been suggested for the Late Maastrichtian

of Zumaia by *Batenburg et al.* [2012], and is similar to the response of sedimentary records to Cenozoic climate forcing [*Pälike et al.*, 2006; *Holbourn et al.*, 2007; *Westerhold et al.*, 2011]. The underlying mechanism that explains this relationship is a globally intensified hydrological cycle during insolation eccentricity maxima that enhances weathering intensity and riverine nutrient and terrestrial organic carbon (lighter $\delta^{13}C_{HCO3}$-) supply to the ocean. Model simulations of the carbon-isotope response to 405 kyr climate variability during the Miocene climatic optimum have shown that a key factor controlling the oceanic $\delta^{13}C$ record was the burial ratio of $CaCO_3$ to organic carbon [*Ma et al.*, 2011]. A net increase in the global burial of $CaCO_3$ at eccentricity maxima (mainly driven by tropical shallow-water carbonates) relative to organic carbon in ocean basins will lead to a decrease in oceanic $\delta^{13}C$, and vice versa. This mechanism is consistent with Option 2 tuning of our Santonian data.

However, relationships between eccentricity cycles and the carbon-isotope record may be more complex than supposed by the above studies, as the seasonal contrasts at insolation highs and lows must also be considered. An important constraint, for instance, would be the quantity of organic carbon stored on land. Eccentricity minima favor less seasonality and thus smaller areas with semi-arid and semi-humid climates. A more even yearly distribution of precipitation enhances organic-carbon burial during pedogenesis and peat formation. In this case, the driver for positive $\delta^{13}C$ excursions during eccentricity minima would be located primarily on land (*Zachos et al.*, 2010).

Previous studies have observed a phase lag in the order of 20 to 60 kyr between insolation 405 kyr eccentricity maxima and 405 kyr minima of carbon-isotope variations [*Pälike et al.*, 2006; *Holbourn et al.*, 2007; *Westerhold et al.*, 2011]. This phase lag is explained by the long residence time of carbon in the ocean, which implies a delayed response to astronomical forcing [*Pälike et al.*, 2006]. A phase lag was most probably also a persistent feature throughout the Cretaceous, but cannot be documented here due to the uncertainties in the

recent Santonian radiometric dates and in the ATS of Seaford Head and of the Niobrara Formation. However, such a phase lag would account for only a very small source of error, and the nearly identical La2010d/La2011 solutions appear as robust astronomical models for the Cretaceous [*Batenburg et al.*, 2012; *Dinarès-Turrell et al.*, 2013, 2014; *Wu et al.*, 2014]. Option 2 appears by far the most likely solution for the astronomical calibration of the Santonian (Fig. 9, Table 2). If, as supported by this option, the near-coincidence between 405 kyr eccentricity maxima of insolation and 405 kyr minima of the oceanic $\delta^{13}C$ can be proven to be a reliable feature of Cretaceous climate, a significant improvement of the Geologic Time Scale could be achieved through high-resolution carbon-isotope stratigraphy, filter extraction of the $\delta^{13}C$ 405 kyr component, and calibration to La2011 by assuming a close to 180° phase relationship to the astronomical solution.

5. Conclusions

New high-resolution carbon-isotope records of bulk carbonate have been correlated across the Upper Coniacian to Lower Campanian intervals in the reference sections of Seaford Head (England) and Bottaccione (Gubbio, central Italy). This study demonstrates an unambiguous stratigraphic correlation of the Santonian–Campanian boundary positive $\delta^{13}C$ excursion to a short distance below the C34N/C33R chron reversal in the Bottaccione (Gubbio) Tethyan reference record, and to the HO of *Marsupites testudinarius* in the Boreal realm. The Santonian–Campanian Boundary Event (SCBE) is characterized by a pronounced double peak at the summit of a medium-term $\delta^{13}C$ maximum, which makes it a reliable stratigraphic marker for the top Santonian.

The new record at Seaford Head constitutes the highest resolution carbon-isotope curve for the uppermost Coniacian to lowermost Campanian interval obtained to date, and reveals the

expression of orbital forcing. Filtering of the 405 kyr eccentricity cycles from the Seaford Head $\delta^{13}C$ curve allows construction of a floating astronomical time scale (ATS) of the Boreal Santonian.

Anchoring of the Seaford Head ATS and that of the Niobrara Formation (Western Interior) to the recent radiometric dating of the Santonian–Campanian boundary (84.19±0.38Ma) permits an astronomical calibration of the stage to the La2011 solution. Astronomical calibration allows precise correlation of the Boreal Santonian to the endemic ammonite and inoceramid zones of the Western Interior, and suggests that a slight (c. 200 kyr) mismatch exists in the correlation of the Coniacian–Santonian boundary between the Boreal realm and the Western Interior Basin.

Five tuning options have been examined. Of these five options, Option 2 appears as the most likely and pre-supposes that 405 kyr insolation minima correspond to maxima in the $\delta^{13}C$ of the Chalk sea and *vice versa*. We propose two distinct mechanisms to explain this relationship: (1) similar to previous studies in the Cenozoic, changes in the burial rate of $CaCO_3$ relative to that of organic carbon in oceanic basins, caused by climate forcing of weathering, drove changes in nutrient input and oceanic productivity, which played a key role in controlling global $\delta^{13}C$; (2) the difference in seasonal contrasts between insolation lows and highs caused significant differences in organic-carbon burial on land.

Acknowledgments

N. Thibault warmly thanks Mathieu Martinez for fruitful discussions on cyclostratigraphy and the Mærsk Oil Cross Disciplinary Chalk Center (C3) for funding. K. Attree acknowledges support by Kingston University London for a part-time PhD

studentship. We thank Norman Charnley for analyzing the Seaford Head and some of the Gubbio samples in the Oxford isotope laboratory. All data are available in the supporting information.

References

Barchi, P. (1995), Géochimie et magnétostratigraphie du Campanien de l'Europe du Nord-Ouest. PhD Thesis, Université Pierre et Marie Curie, Paris 06. 288 p.

Batenburg, S.J., Sprovieri, M., Gale, A.S., Hilgen, F.J., Hüsing, S., Laskar, J., Liebrand, D., Lirer, F., Orue-Etxebarria, X., Pelosi, N., and J. Smit (2012), Cyclostratigraphy and astronomical tuning of the Late Maastrichtian at Zumaia (Basque country, Northern Spain). Earth Planet. Sci. Lett., 359–360, 264–278

Birkelund, T., Hancock, J.M., Hart, M.B., Rawson, P.F., Remane, J., Robaszynski, F., Schmid F., and F. Surlyk (1984), Cretaceous stage boundaries. Bull. Geol. Soc. Denmark, 33, 3–20.

Bosmans, J.H.C., Hilgen, F.J., Tuenter, E., and L.J. Lourens (2015). Obliquity forcing of low-latitude climate. Clim. Past 11, 1335–1346, doi:10.5194/cp-11-1335-2015

Burnett, J.A., Gallagher, L.T., and M.J. Hampton (1998), Upper Cretaceous, in: Calcareous Nannofossil Biostratigraphy, edited by P.R. Bown, pp. 132–199, Kluwer, Dordrecht.

Coccioni, R., and I. Premoli Silva (2015), Revised Upper Albian–Maastrichtian planktonic foraminiferal biostratigraphy and magnetostratigraphy of the classical Tethyan Gubbio section (Italy). Newslett. Stratigr., 48, 47–90.

Dinarès-Turrell, J., Pujalte, V., Stoykova, K., and J. Elorza (2013), Detailed correlation and astronomical forcing within the Upper Maastrichtian succession in the Basque Basin. Bol. Geol. Miner., 124, 253–282.

Dinarès-Turrell, J., Westerhold, T., Pujalte, V., Röhl, U., and D. Kroon (2014), Astronomical calibration of the Danian stage (Early Paleocene) revisited: Settling chronologies of sedimentary records across the Atlantic and Pacific Oceans. Earth. Planet. Sci. Lett., 405, 119–131.

Fritsen, A. (1999), A Joint Chalk Stratigraphic Framework. Volume 1. Joint Chalk Research Program Topic V. Norwegian Petroleum Directorate, 206p.

Gale, A.S., Montgomery, P., Kennedy, W.J., Hancock, J.M., Burnett, J.A., and J.M. McArthur (1995), Definition and global correlation of the Santonian–Campanian boundary. Terra Nova, 7, 611–622.

Gale, A.S., Hancock, J.M., Kennedy, W.J., Petrizzo, M.R., Lees, J.A., Walaszczyk, I., and D.S. Wray (2008), An integrated study (geochemistry, stable oxygen and carbon isotopes, nannofossils, planktonic foraminifera, inoceramid bivalves, ammonites and crinoids) of the Waxahachie Dam Spillway section, north Texas: a possible boundary stratotype for the base of the Campanian Stage. Cretaceous Res., 29, 131–167.

Gardin, S., Del Panta, F., Monechi, S., and M. Pozzi (2001), A tethyan reference record for the Campanian and Maastrichtian stages: the Bottaccione section (Central Italy); review of the data and new calcareous nannofossil results, in: The Campanian–Maastrichtian Stage Boundary. Characterisation at Tercis les Bains (France) and Correlation with Europe and other continents, Developments in Palaeontology and Stratigraphy Series, vol. 19, edited by G.S. Odin, pp. 745–757, Elsevier, Amsterdam.

Gardin, S., Galbrun, B., Thibault, N., Coccioni, R., and I. Premoli-Silva (2012), Bio-magnetochronology for the upper Campanian Maastrichtian from the Gubbio area, Italy: new results from the Contessa Highway and Bottaccione sections. Newslett. Stratigr., 45, 75–103.

Gradstein, F., Ogg, J., Schmitz, M., and G. Ogg (Eds.) (2012), The Geologic Time Scale 2012. Elsevier, Boston, USA, doi: 10.1016/B978-0-444-59425-9.00004-4.

Hampton, M.J., Bailey, H.W., Gallagher, L.T., Mortimore, R.N., and C.J. Wood (2007), The biostratigraphy of Seaford Head, Sussex, southern England; an international reference section for the basal boundaries for the Santonian and Campanian Stages in chalk facies. Cretaceous Res., 28, 43–60.

Hancock, J.M., and A.S. Gale (1996), The Campanian Stage. In: Rawson, P.F., Dhondt, A.V., Hancock, J.M., and W.J. Kennedy (Eds.), Proceedings ‘‘Second International Symposium on Cretaceous Stage Boundaries’’, Brussels, September 1995. Bulletin de l’Institut Royal des Sciences Naturelles de Belgique, Sciences de la Terre, 66 (Supplement), 103–109.

Holbourn, A., Kuhnt, W., Schulz, M., Flores, J.A., and N. Andersen (2007), Orbitally-paced climate evolution during the middle Miocene. Earth Planet. Sci. Lett., 261, 534–550.

Holden, N.E., Bonardi, M.L., De Bièvre, P., Renne, P.R., and I.M. Villa (2011), IUPAC-IUGS common definition and convention on the use of the year as a derived unit of time (IUPAC-IUGS Recommendations 2011). Episodes, 34, 39–40.

Husson, D., Thibault, N., Galbrun, B., Gardin, S., Minoletti, F., Sageman, B., and E. Huret (2014), Lower Maastrichtian cyclostratigraphy of the Bidart section (Basque country,

SW France): a remarkable record of precessional forcing. Palaeogeogr. Palaeoclimatol. Palaeoecol., 395, 176–197.

Jarvis, I., Mabrouk, A., Moody, R.T.J., and S. de Cabrera (2002), Late Cretaceous (Campanian) carbon isotope events, sea-level change and correlation of the Tethyan and Boreal realms. Palaeogeogr., Palaeoclimatol., Palaeoecol., 188, 215–248.

Jarvis I., Gale A.S., Jenkyns H.C., and M.A. Pearce (2006), Secular variation in Late Cretaceous carbon isotopes: a new $\delta^{13}C$ carbonate reference curve for the Cenomanian–Campanian (99.6–70.6 Ma). Geol. Mag., 143, 561–608.

Jarvis, I., Mabrouk, A., Moody, R.T.J., Murphy, A.M., and R.I. Sandman (2008), Applications of carbon isotope and elemental (Sr/Ca, Mn) chemostratigraphy to sequence analysis: sea-level change and the global correlation of pelagic carbonates, in: Geology of East Libya, edited by Salem, M.J., and A.S. El-Hawat, pp. 369–396, Earth Science Society of Libya, Tripoli.

Jarvis I., Trabucho-Alexandre, J., Gröcke, D.R., Uličný, D., and J. Laurin (2015), Stable-isotope chemostratigraphy: intercontinental correlation of organic carbon and carbonate records, and evidence of climate and sea-level change during the Turonian (Cretaceous). The Depositional Record, 1, 53–90, doi: 10.1002/dep2.6.

Jenkyns, H.C., Gale, A.S., and R.M. Corfield (1994), Carbon- and oxygen-isotope stratigraphy of the English Chalk and Italian Scaglia and its palaeoclimatic significance. Geol. Mag., 131, 1–34.

Joo, Y.J., and B.B. Sageman (2014), Cenomanian to Campanian carbon isotope chemostratigraphy from the Western Interior Basin, U.S.A. J. Sediment Res., 84, 529–542.

Lamolda, M.A., and J.M. Hancock (1996), The Santonian Stage and substages. In: Rawson, P.F., Dhondt, A.V., Hancock, J.M., and W.J. Kennedy (Eds.), Proceedings, ‘‘Second International Symposium on Cretaceous Stage Boundaries’’, Brussels, September 1995. Bulletin de l’Institut Royal des Sciences Naturelles de Belgique, Sciences de la Terre, 66 (Supplement), 95–102.

Lamolda, M.A., Paul, C.R.C, Peryt, D., and J.M. Pons (2014), The Global Boundary Stratotype and Section Point (GSSP) for the base of the Santonian Stage, “Cantera de Margas”, Olazagutia, northern Spain. Episodes, 37, 1–13.

Laskar, J., Robutel, P., Joutel, F., Gastineau, M., Correia, A., and B. Levrard (2004), A long term numerical solution for the insolation quantities of the earth. Astron. Astrophys., 428, 261–285.

Laskar, J., Fienga, A., Gastineau, M., and H. Manche (2011a), La2010: a new orbital solution for the long-term motion of the Earth. Astron. Astrophys., 532, A89, doi:10.1051/0004-6361/201116836.

Laskar, J., Gastineau, M., Delisle, J.-B., Farrés, A., and A. Fienga (2011b), Strong chaos induced by close encounters with Ceres and Vesta. Astron. Astrophys., 532, L4, doi:10.051/0004-6361/201117504.

Laurin, J., Meyers, S.R., Ulicny, D., Jarvis, I., and B.B. Sageman (2015), Axial obliquity control on the greenhouse carbon budget through middle- to high-latitude reservoirs. Paleoceanography, 30, doi:10.1002/2014PA002736.

Locklair, R.E., and B.B. Sageman (2008), Cyclostratigraphy of the Upper Cretaceous Niobrara Formation, Western Interior, U.S.A.: a Coniacian–Santonian orbital timescale. Earth Planet. Sci. Lett., 269, 539–552.

Ma, W., Tian, J., Li, Q., and P. Wang (2011), Simulation of long eccentricity (400-kyr) cycle in ocean carbon reservoir during Miocene Climate optimum: Weathering and nutrient response to orbital change. Geophys. Res. Lett., 38, L10701, doi:10.1029/2011GL047680.

Meyers, S.R. (2014), Astrochron: An R Package for Astrochronology. http://cran.r-project.org/package=astrochron.

Meyers, S.R., and B.B. Sageman (2007), Quantification of deep-time orbital forcing by average spectral misfit. Am. J. Sci., 307, 773–792.

Meyers, S.R., Sageman, B.B., and L.A. Hinnov (2001), Integrated quantitative stratigraphy of the Cenomanian–Turonian Bridge Creek Limestone Member using Evolutive Harmonic Analysis and stratigraphic modeling. J. Sedim. Res., 71, 628644.

Meyers, S.R., Sageman, B.B., and M.A. Arthur (2012), Obliquity forcing of organic matter accumulation during Oceanic Anoxic Event 2. Paleoceanography, 27, PA3212, doi:10.1029/2012PA002286.

Monechi, S., and H.R. Thierstein (1985), Late Cretaceous—Eocene nannofossil and magnetostratigraphic correlations near Gubbio, Italy. Mar. Micropaleontol., 9, 419–440.

Montgomery, P., Hailwood, E.A., Gale, A.S., and J.A. Burnett (1998), The magnetostratigraphy of Coniacian–Late Campanian chalk sequences in southern England. Earth Planet. Sci. Lett., 156, 209–224.

Mortimore, R.N. (1986), Stratigraphy of the Upper Cretaceous White Chalk of Sussex. Proc. Geol. Assoc., 97, 97–139.

Mortimore, R.N., and B. Pomerol (1987), Correlation of the Upper Cretaceous White Chalk (Turonian to Campanian) in the Anglo-Paris Basin. Proc. Geol. Assoc., 98, 97–143.

Pälike, H., Frazier, J., and J.C. Zachos (2006), Extended orbitally forced palaeoclimatic records from the equatorial Atlantic Ceara Rise. Quatern. Sci. Rev., 25, 3138–3149.

Petrizzo, M.R., Falzoni, F., and I. Premoli Silva (2011), Identification of the base of the lower-to- middle Campanian *Globotruncana ventricosa* zone: Comments on reliability and global correlations. Cretaceous Res., 32, 387–405.

Premoli Silva, I., and W.V. Sliter (1994), Cretaceous planktonic foraminiferal biostratigraphy and evolutionary trends from the Bottaccione Section, Gubbio, Italy. Palaeontogr. Ital., 81, 2–90.

Sageman, B.B., Singer, B.S., Meyers, S.R., Siewert, S.E., Walaszczyk, I., Condon, D.J., Jicha, B.R., Obradovich, J.D., and D.A. Sawyer (2014), Integrating $^{40}Ar/^{39}Ar$, U-Pb, and astronomical clocks in the Cretaceous Niobrara Formation, Western Interior Basin, USA. GSA Bull., 126, 956–973.

Scholle, P.A., and M.A. Arthur (1980), Carbon isotope fluctuations in Cretaceous pelagic limestones: potential stratigraphic and petroleum exploration tool. AAPG Bull., 64, 67–87.

Schulz, M., and M. Mudelsee (2002), REDFIT: estimating red-noise spectra directly from unevenly spaced paleoclimatic time series. Comput. Geosci., 28, 421–426.

Schulz, M.-G., Ernst, G., Ernst, H., and F. Schmid (1984), Coniacian to Maastrichtian stage boundaries in the standard section for the Upper Cretaceous white chalk of NW Germany (Lägerdorf-Kronsmoor-Henmoor): Definitions and proposals. Bull. Geol. Soc. Denmark, 33, 203–215.

Schönfeld, J., Schulz, M.-G., McArthur, J.M., Burnett, J.A., Gale, A.S., Hambach, U., Hansen, H.J., Kennedy, W.J., Rasmussen, K.L., Thirlwall, M.F., and D. Wray, D. (1996), New results on biostratigraphy, paleomagnetism, geochemistry and correlation from the standard section for the Upper Cretaceous White Chalk of northern Germany (Lägerdorf - Kronsmoor - Hemmoor). Mitt. Geol.–Paläontol. Instit. Univ. Hamburg, 77, 545–575.

Scotese, C.R. (2014), Atlas of Late Cretaceous Paleogeographic Maps, PALEOMAP Atlas for ArcGIS, volume 2, The Cretaceous, Maps 16 – 22, Mollweide Projection, PALEOMAP Project, Evanston, IL.

Sprovieri, M., Sabatino, N., Pelosi, N., Batenburg, S.J., Coccioni, R., Iavarone, M., and S. Mazzola (2013), Late Cretaceous orbitally-paced carbon isotope stratigraphy from the Bottaccione Gorge (Italy). Palaeogeogr. Palaeoclimatol.Palaeoecol., 379–380, 81–94.

Taner, M.T. (2000), Attributes Revisited. Technical Publication, Rock Solid Images, Inc., Houston, Texas. URL: http://www.rocksolidimages.com/pdf/attrib_revisited.htm.

Tessin, A., Hendy, I., Sheldon, N., and B.B. Sageman (2015), Redox-controlled preservation of organic matter during “OAE3” within the Western Interior Seaway. Paleoceanography, 30, doi: 10.1002/2014PA002729.

Thibault, N., Husson, D., Harlou, R., Gardin, S., Galbrun, B., Huret, E., and F. Minoletti (2012a), Astronomical calibration of upper Campanian–Maastrichtian carbon isotope events and calcareous plankton biostratigraphy in the Indian Ocean (ODP Hole 762C): Implication for the age of the Campanian–Maastrichtian boundary. Palaeogeogr. Palaeoclimatol. Palaeoecol., 337–338, 52–71.

Thibault, N., Harlou, R., Schovsbo, N., Schiøler, P., Minoletti, F., Galbrun, B., Lauridsen, B.W., Sheldon, E., Stemmerik, L., and F. Surlyk (2012b), Upper Campanian–Maastrichtian nannofossil biostratigraphy and high-resolution carbon-isotope stratigraphy of the Danish Basin: towards a standard δ13C curve for the Boreal Realm. Cretaceous Res., 33, 72–90.

Voigt, S., Friedrich, O., Norris, R.D., and J. Schönfeld (2010), Campanian – Maastrichtian carbon isotope stratigraphy: shelf-ocean correlation between the European shelf sea and the tropical Pacific Ocean. Newslett. Stratigr., 44, 57–72.

Voigt, S., Gale, A.S., Jung, C., and H.C. Jenkyns (2012), Global correlation of Upper Campanian – Maastrichtian successions using carbon-isotope stratigraphy: development of a new Maastrichtian timescale. Newslett. Stratigr., 45, 25–53.

Wagreich, M. (2012), "OAE 3" – regional Atlantic organic carbon burial during the Coniacian–Santonian. Clim. Past, 8, 1447-1455, doi:10.5194/cp-8-1447-2012.

Westerhold, T., Röhl, U., Donner, B., McCarren, H.K., and J.C. Zachos (2011), A complete high-resolution Paleocene benthic stable isotope record for the central Pacific (ODP Site1209). Paleoceanography, 26, PA2216, doi:10.1029/2010PA002092.

Wu, H., Zhang, S., Hinnov, L.A., Jiang, G., Yang, T., Li, H., Wan, X., and C. Wang (2014), Cyclostratigraphy and orbital tuning of the terrestrial upper Santonian-Lower Danian in Songliao Basin, northeastern China. Earth Planet. Sci. Lett., 407, 82–95.

Zachos, J.C., McCarren, H., Murphy, B., Röhl, U., and T. Westerhold (2010), Tempo and scale of late Paleocene and early Eocene carbon isotope cycles. Earth Planet. Sci. Lett., 299, 242–249.

Zeebe, R. E., and D.A. Wolf-Gladrow (2008), Carbon dioxide, dissolved (ocean). In: Gornitz, V. (Ed.), Encyclopedia of Paleoclimatology and Ancient Environments, Kluwer Academic Publishers, Earth Science Series.

Figure Captions

Figure 1. Paleogeography of the Western Interior, North Atlantic, Chalk sea and western Tethys during the Santonian (at 86 Ma), with locations of: (1) English Chalk sections; (2) Lägerdorf, North Germany; (3) Gubbio sections, Italy; (4) sections of the Niobrara Formation, U.S. Western Interior. After *Scotese* [2014]; Mollweide projection with a sea level of +80 m.

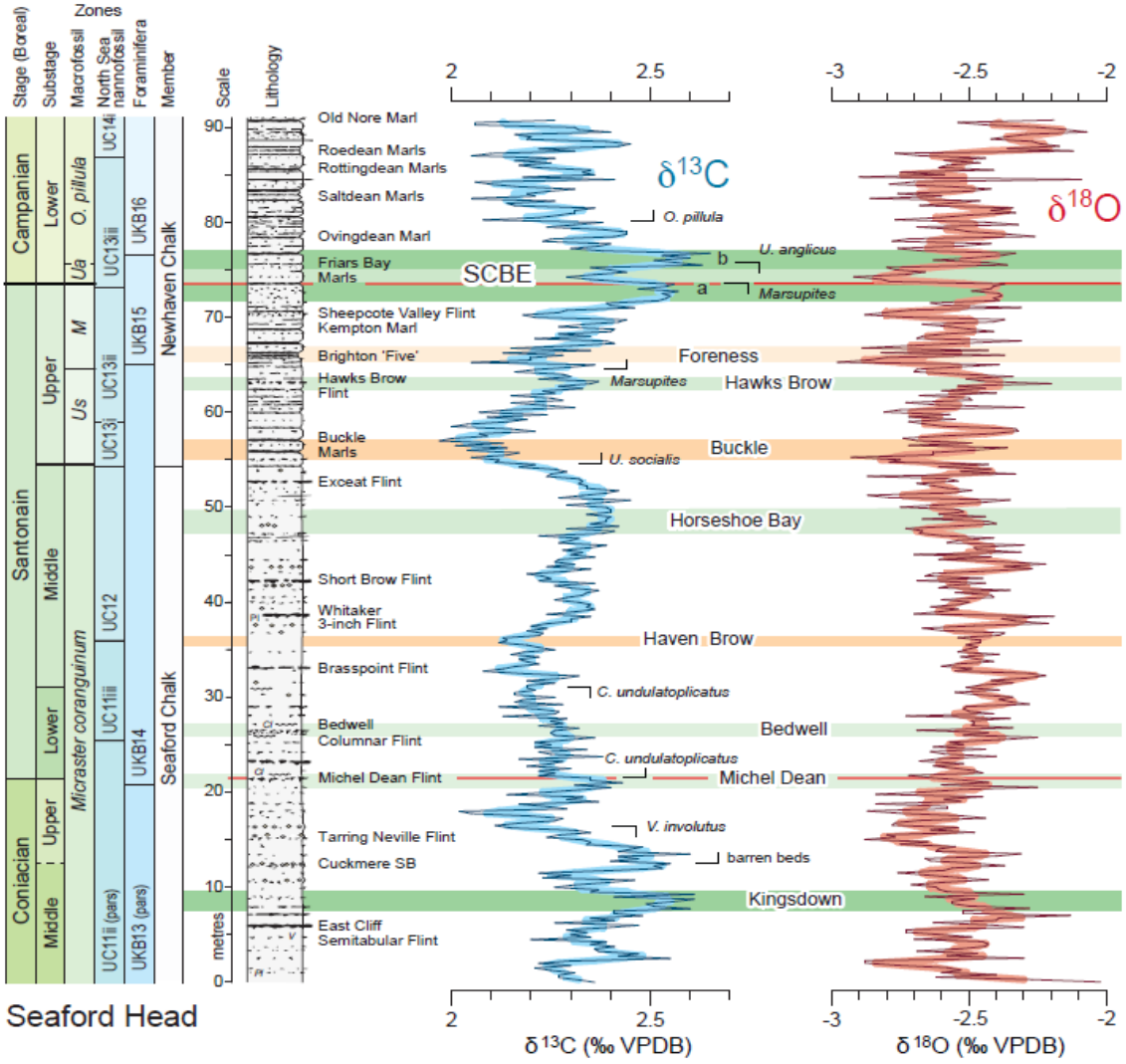

Figure 2. Summary log of the Middle Coniacian to lowermost Campanian at Seaford Head with bulk carbonate carbon and oxygen stable-isotope profiles. The thin blue (carbon) and red (oxygen) lines join isotopic data points for 25 cm-interval samples; the thick underlying curves correspond to a 3-point running averages. Lithological log and carbon-isotope events after *Jarvis et al.* [2006]; SCBE = Santonian–Campanian Boundary Event. Macrofossil biostratigraphy and datum levels are from this study; stage and substage boundaries are placed based on our macrofossil records from the section. Micro- and nannofossil biostratigraphy modified (see text) from *Hampton et al.* [2007]. Marker bed terminology modified from *Mortimore* [1986, 1997]. See Appendix 1 for further information and key.

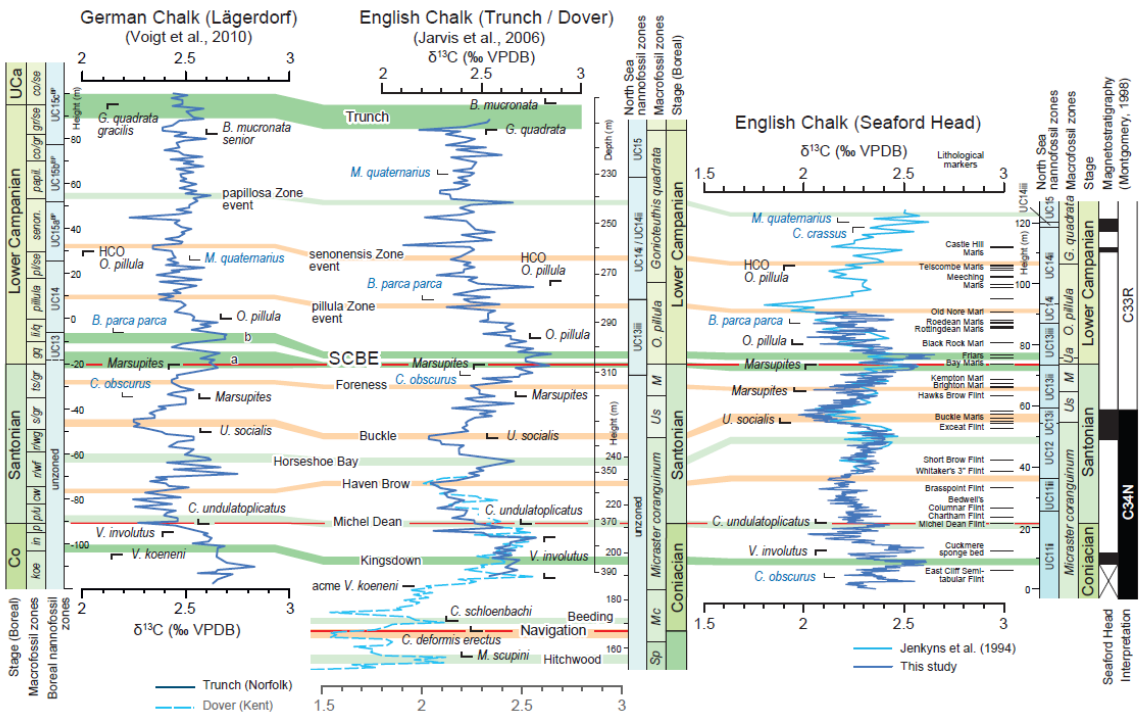

Figure 3. Correlation of Boreal carbon-isotope records from Lägerdorf (North Germany), Trunch/Dover (England) and Seaford Head (England). Lägerdorf stratigraphy and isotope data after *Schönfeld et al.* [1996] and *Voigt et al.* [2010]. Trunch and Dover data from *Jenkyns et al.* [1994] and *Jarvis et al.* [2006]. The high-resolution (25 cm interval) carbon-isotope record from Seaford Head (this study) and low-resolution data (1 m spacing) of *Jenkyns et al.* [1994] are compared to the macrofossil (this study), nannofossil (modified from *Hampton et al.* [2007]), and magnetostratigraphy [*Montgomery et al.*, 1998] of the section. Carbon-isotope events after *Jarvis et al.* [2006] and this paper; SCBE = Santonian – Campanian Boundary Event. Lägerdorf macrofossil zone names detailed in *Schönfeld et al.* [1996]; HCO = highest common occurrence, *M* = *Marsupites*, *Mc* = *Micraster cortestudinarium*, *Sp* = *Sternotaxis plana*, *Ua* = *Uintacrinus anglicus*, *Us* = *Uintacrinus socialis*.

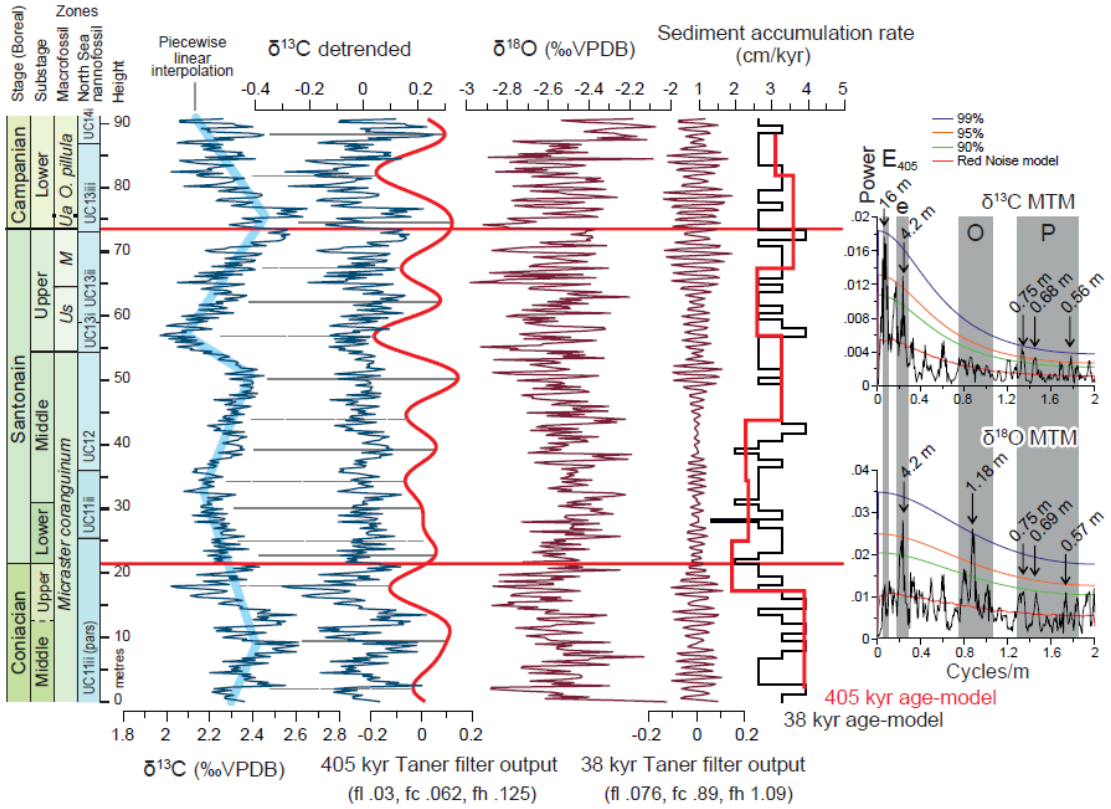

Figure 4. Cyclostratigraphy of bulk carbonate carbon and oxygen stable-isotope records of Seaford Head in the depth domain. Periodograms on the right side of the figure correspond to 4 pi Multi-Taper Method (MTM) power spectra. Compacted sediment accumulation rates are derived from two distinct age-models based on the 405 kyr and 38 kyr filtering of the $\delta^{13}C$ and $\delta^{18}O$ records, respectively.

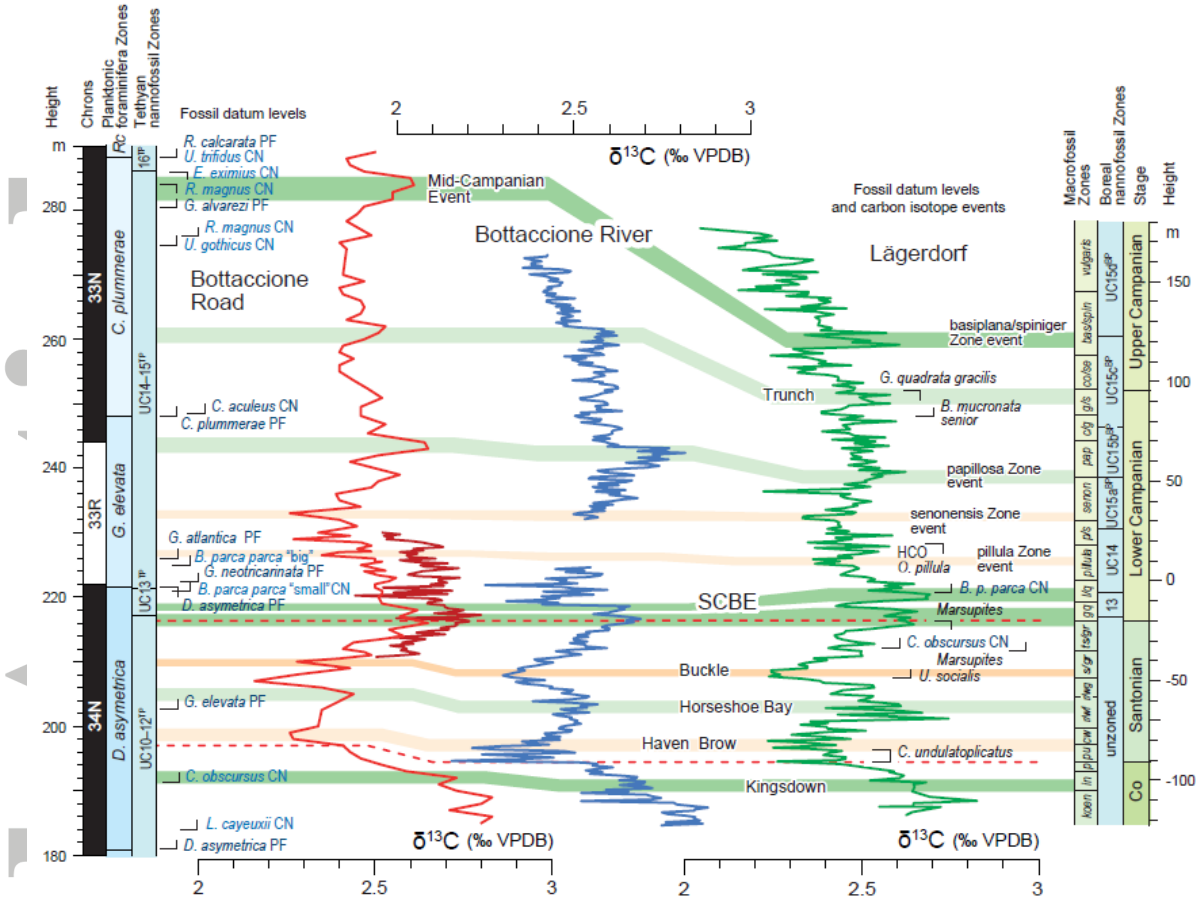

Figure 5. Correlation of new carbon-isotope records of the Bottaccione Road and Bottaccione River sections to the $\delta^{13}C$ curve of Lägerdorf (North Germany). Magneto- and biostratigraphy of the Bottaccione section from *Coccioni and Premoli-Silva* [2015]. The base of UC14 is defined here by the LO of "small" *B. parca parca* (<10µm) [*Gardin et al.*, 2001]. Lägerdorf macrofossil biostratigraphy and datum levels after *Schönfeld et al.* [1996]; calcareous nannofossil zonation from *Voigt et al.* [2010] after *Burnett et al.* [1998]; carbon isotopes from *Voigt et al.* [2010]. Carbon-isotope events after *Jarvis et al.* [2002, 2006] and this study.

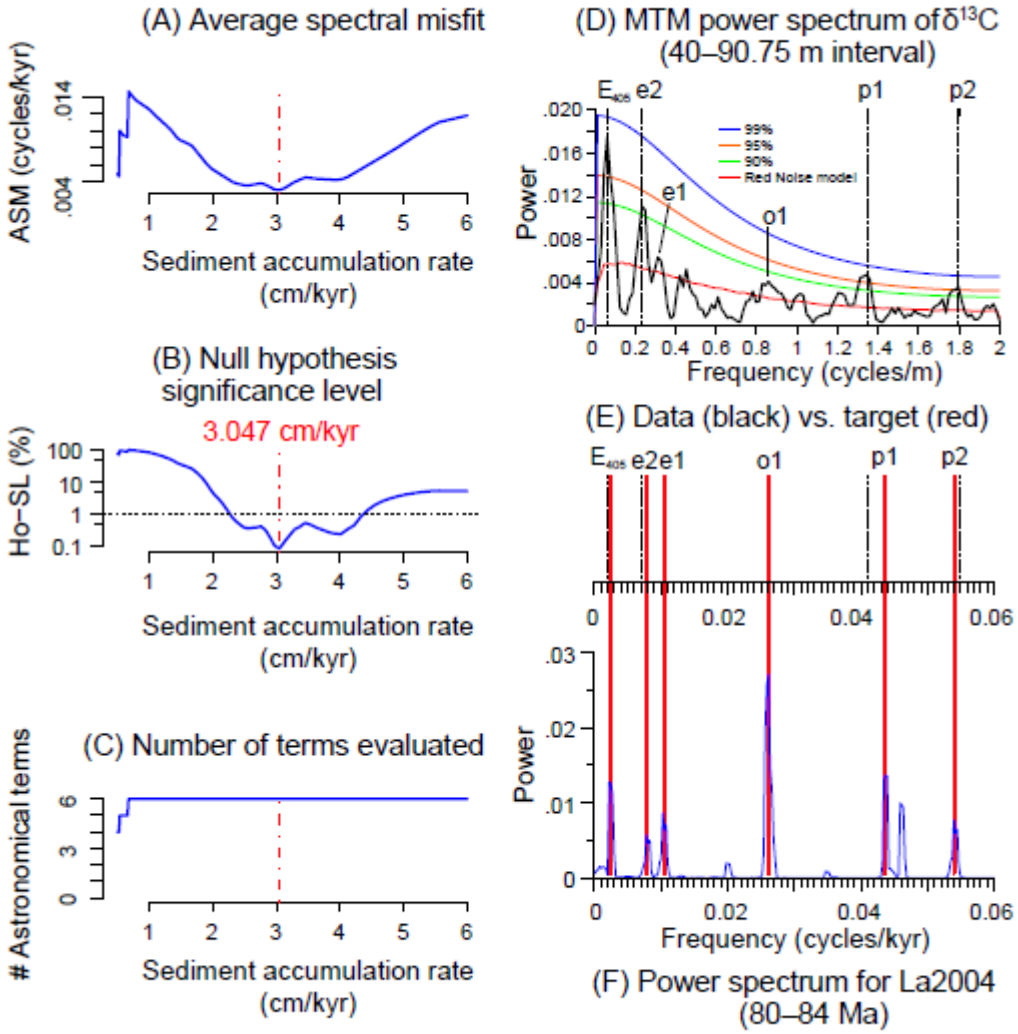

Figure 6. Results of the Average Spectral Misfit method (ASM) for the $\delta^{13}C$ time-series of the 40 to 90.75 m interval. The evaluated orbital terms of the Laskar solution [*Laskar et al.*, 2004] are E405, e1, e2, o1, p1 and p2 (see Table 1). (A) Average spectral misfit. (B) Null hypothesis significance level. (C) Number of terms evaluated. (D) Multi-Taper Method (MTM) power spectrum of bulk carbonate $\delta^{13}C$. (E) Data (black) versus target (blue). (F) Power spectra for La2004 (80 – 84 Ma).

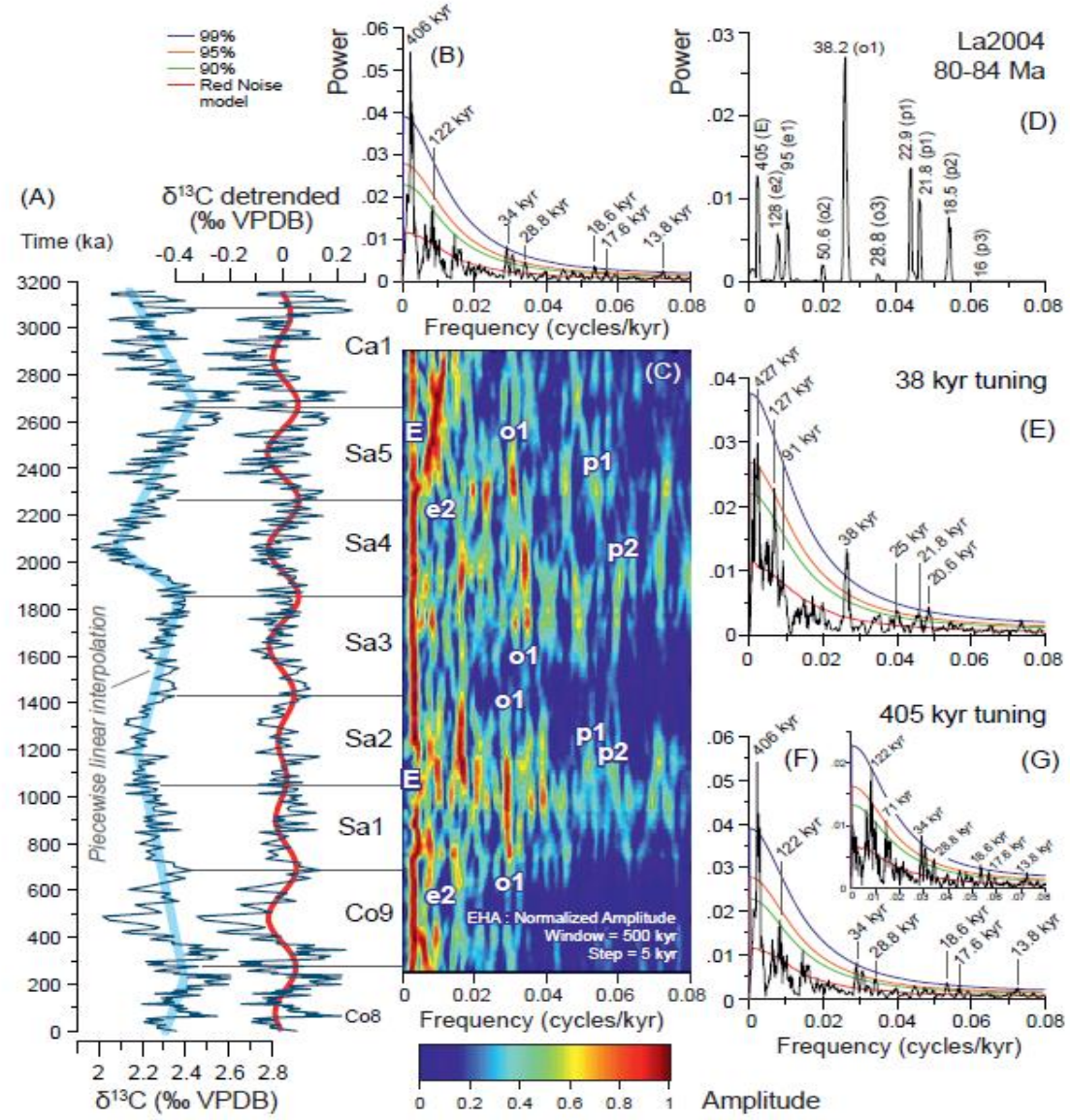

Figure 7. Carbon-isotope record of Seaford Head tuned to 405 kyr cycles and cyclostratigraphic results in the time domain. (A) Primary and detrended $\delta^{13}C$ records with identified cycles. (B) 4 pi Multi-Taper Method (MTM) power spectrum with AR1 confidence level estimates of the 405 kyr tuned $\delta^{13}C$ time-series with power on a logarithmic scale. (C) Normalized amplitude of an Evolutive Harmonic Analysis (EHA) of the 405 kyr tuned $\delta^{13}C$ time-series showing linearity of the E405 kyr component and additional Milankovitch frequencies (e2, o1, p1, p2) expressed mainly in the time intervals from 250 to 1400 ka and from 2100 to 2900 ka. (D) 4 pi MTM of the La2004 astronomical solution for the 80 to 84 Ma interval. (E) 4 pi MTM power spectrum of the 38 kyr tuned $\delta^{13}C$ time-series. (F) 4 pi MTM power spectrum of the 405 kyr tuned $\delta^{13}C$ time-series. (G) 4 pi MTM power spectrum of the 405 kyr tuned $\delta^{13}C$ time-series when the 405 kyr is filtered out.

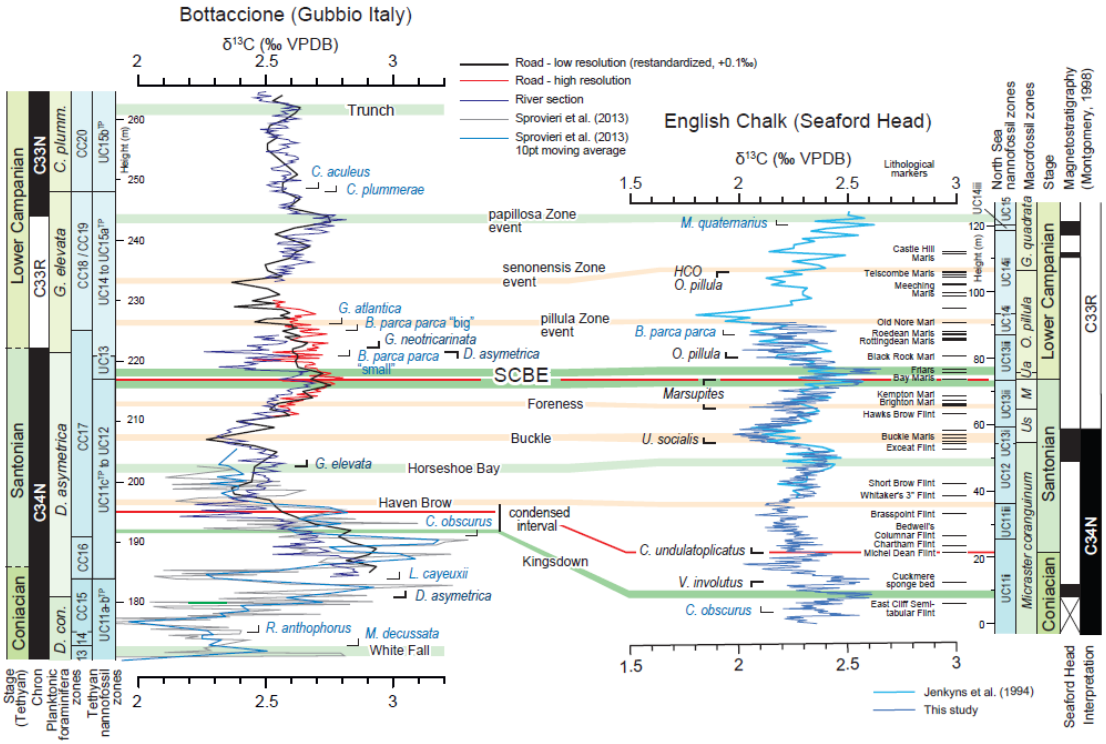

Figure 8. Correlation of Coniacian to Lower Campanian $\delta^{13}C$ records of the Bottaccione (Gubbio, Italy) and Seaford Head (English chalk). Stratigraphy of the Bottaccione section from *Coccioni and Premoli-Silva* [2015] with Coniacian–Santonian carbon-isotope data of *Sprovieri et al.* [2013] plotted for comparison. Seaford Head sources as in Figures 2 and 3.

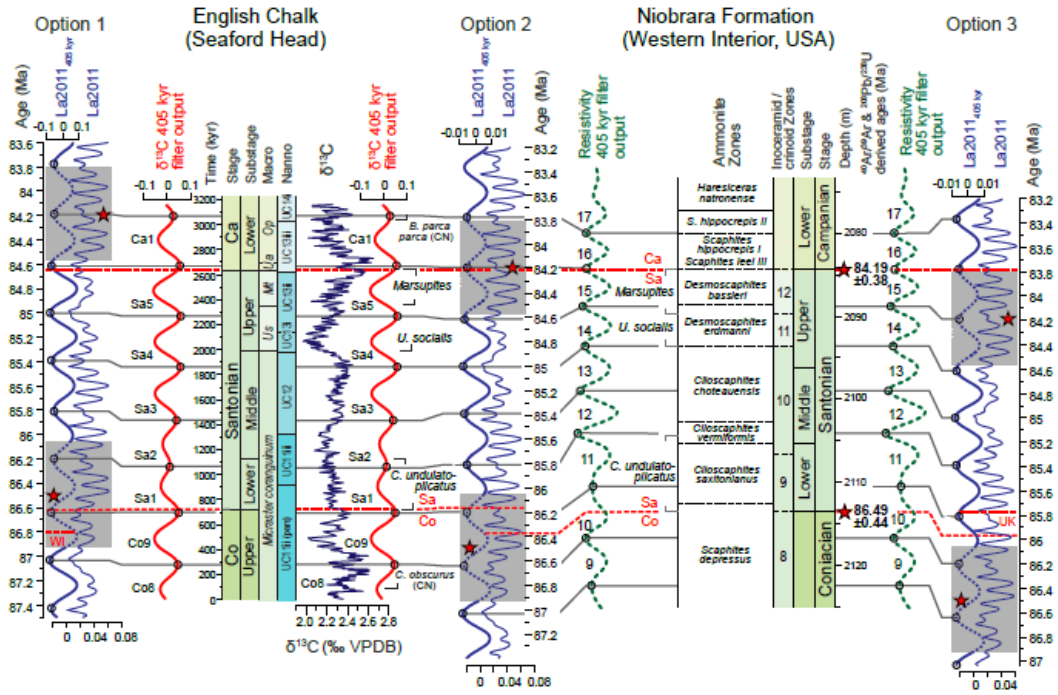

Figure 9. Astronomical tuning to the La2011 solution [*Laskar et al.*, 2011b] of the Seaford Head bulk carbonate carbon isotopes ($\delta^{13}C_{carb}$) tuned to 405 kyr eccentricity cycles and to the floating astronomical time scale of the Niobrara Formation. Tuning options considered here correlate 405 kyr insolation minima to maxima of the Seaford Head $\delta^{13}C_{carb}$ and minima of the resistivity signal in the Niobrara Formation. Seaford Head stratigraphy as in Fig. 2. Niobrara Formation cyclostratigraphy after *Locklair and Sageman* [2008]; radiometric age determinations (highlighted by the red stars) and placement of biostratigraphic zone boundaries after *Sageman et al.* [2014]. Inoceramid /crinoid zones: 8 *Magadiceramus crenelatus*; 9 *Cladoceramus undulatoplicatus*; 10 *Cordiceramus bueltenensis*; 11 *Cordiceramus muelleri*; 12 *Marsupites testudinarius*. Macrofossil LO and HO datum levels plotted relative to the cyclostratigraphy and ammonite zones, based on data presented by *Gale et al.* [1995] and *Locklair and Sageman* [2008]. Ca = Campanian, Co = Coniacian, Sa = Santonian. The grey areas in the La2011 astronomical solution highlight the total range in uncertainty of the radiometric datings.

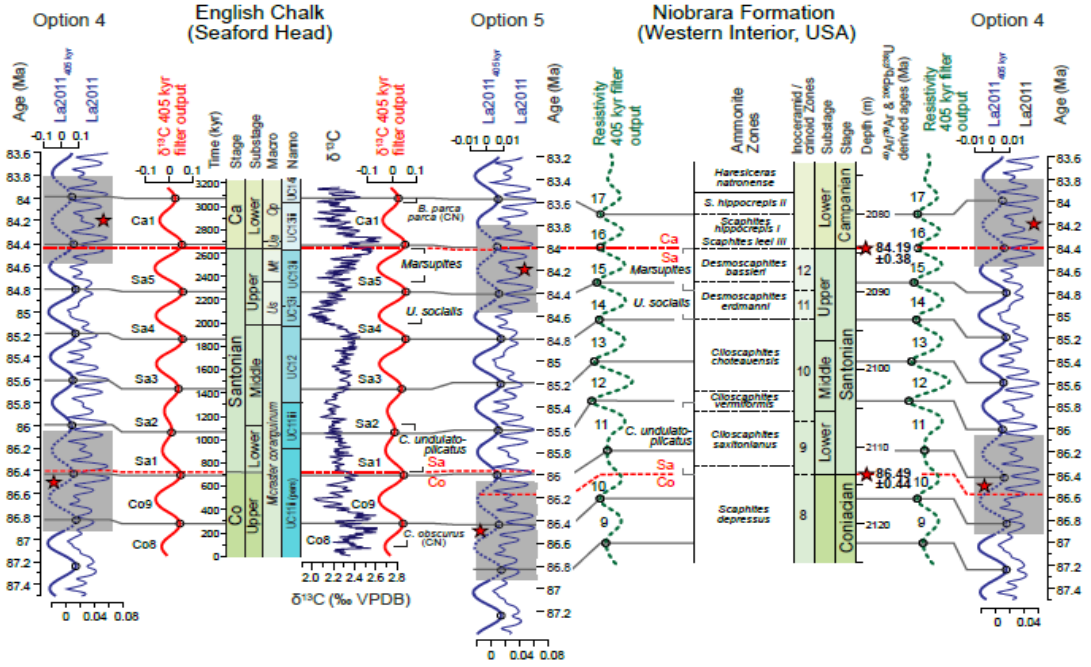

Figure 10. Astronomical tuning to the La2011 solution [*Laskar et al.*, 2011b] of the Seaford Head bulk carbonate carbon isotopes ($\delta^{13}C_{carb}$) tuned to 405 kyr eccentricity cycles and to the floating astronomical time scale of the Niobrara Formation. Tuning options considered here correlate 405 kyr insolation maxima to maxima of the Seaford Head $\delta^{13}C_{carb}$ and minima of the resistivity signal in the Niobrara Formation. Seaford Head stratigraphy as in Fig. 2. Niobrara Formation cyclostratigraphy after *Locklair and Sageman* [2008]; radiometric age determinations (highlighted by the red stars) and placement of biostratigraphic zone boundaries after *Sageman et al.* [2014]. Inoceramid /crinoid zones: 8 *Magadiceramus crenelatus*; 9 *Cladoceramus undulatoplicatus*; 10 *Cordiceramus bueltenensis*; 11 *Cordiceramus muelleri*; 12 *Marsupites testudinarius*. Macrofossil LO and HO datum levels plotted relative to the cyclostratigraphy and ammonite zones, based on data presented by *Gale et al.* [1995] and *Locklair and Sageman* [2008]. Ca = Campanian, Co = Coniacian, Sa = Santonian. The grey areas in the La2011 astronomical solution highlight the total range in uncertainty of the radiometric dating.

Table 1. Orbital targets of the La2004 astronomical solution [*Laskar et al.*, 2004] for the 80 to 84 Ma interval and their uncertainty with assignment of the observed frequencies of the $\delta^{13}C$ time-series to these orbital terms. Percentage uncertainties in frequency of the orbital terms are those provided by *Meyers et al.* [2012] for the Cenomanian–Turonian interval.

Term	La2004 period (kyr)	% uncertainty in frequency	observed frequency (cycles/m)	Chi-2 significance
E405	405	2.3%	**0.0625**	**>95%**
e2	128	4.6%	**0.2344**	**>90%**
e1	95	4.2%	0.3125	<85%
e3	76.9	4%	0.4531	<85%
o2	50.6	1.6%	0.6094	<AR1 base level
o1	38.2	0.8%	0.8954	<85%
p1	22.9	3.5%	**1.344**	**>95%**
p2	18.5	0.4%	**1.797**	**>95%**

Table 2. Radiometric ages for Santonian stage boundaries and ages derived from the projection of the Coniacian–Santonian and Santonian–Campanian boundaries as defined by their biostratigraphic criteria when considering the 5 different tuning options to the La2011 astronomical solution.

Defining criteria of the Santonian stage	Radiometric age , Ma [*Sageman et al.*, 2014]	La2011 (Ma) option 1	La2011 (Ma) option 2	La2011 (Ma) option 3	La2011 (Ma) option 4	La2011 (Ma) option 5
Sa/Ca (LO*Marsupites*)	84.19±0.38	84.65	84.20	83.78	84.44	84.00
Co/Sa (FO*C. undulato- plicatus*) UK		86.62	86.16	85.77	86.4	85.96
Co/Sa (FO*C. undulato- plicatus*) WI	86.49±0.44	86.8	86.37	85.97	86.57	86.17

Figure S1. Detailed log of the Seaford Head section with bulk carbonate carbon and oxygen isotopes and SH samples (red numbers) of *Hampton et al.* [2007] recalibrated to the log. Stratigraphy and data sources as in Fig. 2. Small black filled circles are isotope sample positions. Yellow arrows and black text are macrofossil lowest occurrence (LO) and highest occurrence (HO) datum levels; dark blue are foraminifera; pale blue are calcareous nannofossils.

Figure S2. Results of the Average Spectral Misfit method (ASM) for the $\delta^{13}C$ time-series of the 40 to 90.75 m interval using all observed frequency peaks of the 4 pi Multi-Taper Method (MTM) power spectrum. (A) Average spectral misfit. (B) Null hypothesis significance level. (C) Number of terms evaluated. (D) MTM power spectrum of $\delta^{13}C$. (E) Data versus target frequencies, and (F) Power spectrum for La2004 (80 – 84 Ma). The evaluated orbital terms of the Laskar2004 solution [*Laskar et al.*, 2004] are E405, e2, e1, e3, o2, o1, p1 and p2 (see Table 1).

Figure S3. Results of the Evolutive Harmonic Analysis (EHA) for the $\delta^{13}C$ time-series at Seaford Head in the depth domain. (A) Bulk carbon isotope profile with corresponding detrended curve and 405 kyr Taner filtered output. (B) 4 pi MTM power spectrum. (C) EHA normalized amplitude. (D) EHA probability.

Figure S4. Results of the Evolutive Harmonic Analysis (EHA) for the $\delta^{13}C$ time-series at Seaford Head tuned to 405 kyr cycles. (A) Tuned bulk carbon isotope profile with corresponding detrended curve and 405 kyr filtered output. (B) 405 kyr tuned MTM power spectrum. (C) EHA normalized amplitude. (D) EHA probability.

Figure S5. Results of the Evolutive Harmonic Analysis (EHA) for the $\delta^{13}C$ time-series at Seaford Head tuned to 38 kyr cycles. (A) Tuned bulk carbon isotope profile with

corresponding detrended curve and 38 kyr filtered output. (B) 38 kyr tuned 4 pi MTM power spectrum. (C) EHA normalized amplitude. (D) EHA probability.

Table S1. Table of macro-, micro- and nannofossil datum levels in the Seaford Head section, along with biozonations and lithostratigraphy.

Table S2. Bulk carbonate carbon and oxygen stable isotope data for the Bottaccione River and Road sections.

Table S3. Bulk carbonate carbon and oxygen stable isotope data for the Seaford Head section.